EFFECT OF HEAT TREATMENT ON THE DUCTILE FRACTURE CHARACTERISTICS OF Zr-2.5 Wt. % Nb.

P. F. Timmins *

An experimental investigation using standard J-resistance curves and crictical crack length determinations to examine the effect of four heat-treatments on the toughness behaviour of 17 mm compact specimens of the Zr-2.5 wt. % Nb alloy (Zr-Nb) used for power reactor components, specifically pressure tubes.

A powerful design guide evolved which predicted the critical crack length of pressure tube from a knowledge of the void diameter in the stable crack growth region in small-scale specimens of Zr-Nb, subjected to various heat-treatments.

INTRODUCTION

The alloy Zr-2.5 wt. % Nb (Zr-Nb) is currently used for pressure tubes in power reactors and consequently much attention has been paid to the toughness behaviour of this material, particularly crack initiation toughness J_{IC} , crack propagation toughness and the critical crack length of pressure tubes [1-6].

Further, the use of "characteristic features and distances" in the microstructures of such alloys is receiving more attention as reasearchers attempt to find real physical meaning to energy parameters derived from the toughness of metals which exhibit elastic-plastic behaviour [7,8,9]. The work of Firrao [10] is perceived to be of particular significance in terms of the concept of the "major void" size in relating microstructural features to the mechanism of ductile fracture.

* 233,Timberlane Drive,Abbotsford,
British Colombia,Canada

Accordingly, the present work focuses on the relationships between fracture toughness, critical crack length and fracture surface characteristics derived from heat treated Zr-Nb, 17 mm compact specimens [9].

EXPERIMENTAL PROCEDURE

17 mm compact specimens were machined from 4 mm thick Zr-Nb plate containing 35 ppm hydrogen such that their notches were parallel to the rolling direction. Round tensile specimens of 3.4 mm gage diameter were machined transverse to the rolling direction. The specimens were subjected to the following heat treatments in vacuum, prior to testing.

1. 30% Cold Work + 24 h at 673 K fast cool - "as received" condition.

2. Furnace cooled after 30 minutes at 1123 K.

3. Water quenched after 10 minutes at 1273 K + 24 h at 773 K furnace cooled.

4. Water quenched after 10 minutes at 1143 K + 24 h at 773 K furnace cooled.

Tensile tests were carried out at 298 K at a strain rate of 10^{-4} sec^{-1} ; the compact specimens were fatigue-cracked prior to testing at 298 K, and J-resistance (J-R) curves were produced in accord with A.S.T.M. E813 [11], taking σ_y in the calculations as the 0.2% offset yield stress from the tensile tests. Crack growth was monitored by the potential drop technique [12]. The compacts were post-fatigue cracked to mark the extent of the stable crack growth and to provide clean surfaces for examination by scanning electron microscopy (SEM). Sections were cut through the stable crack growth region for examination of the fracture profile by optical microscopy. Measurements of features on the fracture surfaces were made using an image analysis system.

EXPERIMENTAL RESULTS

J-Resistance Curves. The J-R curves for the four heat-treated conditions of Zr-Nb tested are shown in Figure 1. The shape of the curves are in good agreement with those obtained earlier by Chow and Simpson [12] in their work on this material.

Critical Crack Length Estimation. The crack driving force curve of a tube was calculated using the Folias [13] formulation. This calculation is essentially the Dugdale model modified for the stress increase at the crack tip due to the curvature. This formulation has been verified by a large number of experiments [14].

The critical crack length (CCL) of a tube can be estimated by establishing the tangency condition of the J-R curve and the crack driving force curve, as described by Simpson [15].

For an assumed hoop stress of 100 MPa, a wall thickness of 4.2 mm and a diameter of 53.8 mm, all typical values for tubes under power reactor operating conditions, the CCL for tubes in the four heat treated conditions in which the specimens were tested, were plotted against the measured toughness at a stable crack extension of 1.5 mm, Figure 2.

SEM Examination

In the stable crack growth region of all the compact specimens examined, separation was by initial crack tip blunting and stretch zone [9] formation followed by the growth and coalescence of voids.

Measurements were made of the stretch zone width and the mean void diameters of all the compact specimens tested.

Stretch zones were measured with the specimen tilted at 60° to the electron beam, such that the viewing plane and photomicrographs were normal to the stretch zone. Measurements were then taken from the photomicrographs, after distance standards had been photographed at the same angle of tilt, so as to provide an appropriate calibration and ensure accuracy.

Void diameters were measured from photomicrographs taken of the fracture surfaces with the specimens normal to the electron beam. The photomicrograph images were digitized using an IBAS inboard system.

Plots of the crack initiation toughness, J_{IC} against the stretch zone width and the crack growth toughness at 1.5 mm crack extension against the mean void diameter for the four heat treated conditions were produced, Figures 3 and 4.

Optical Microscopy

Sections were cut through the regions of stable crack growth such that the crack profiles could be examined. For each of the four heat treated conditions, an attempt was made to relate the microstructures to features observed on the fracture surfaces.

The microstructures resulting from the four heat-treated conditions investigated were in accord with those reported in a review by Northwood and Lim [16]. That is, the morphology of the $\alpha + \beta$ phases was altered by heat-treatment, particularly in the furnace cooled specimens and the quenched and aged specimens, but the dominant effect was also greatest in the furnace cooled and the quenched and aged specimens.

The section through the stable crack growth region for the furnace cooled specimen and the corresponding fracture surface are shown in Figure 5. The similar sections for the specimen quenched from 1143 K and aged at 773 K are shown in Figure 6. The hydrides formed during heat treatment dominate these microstructures and probably play a key role in the ductile fracture of the specimens.

DISCUSSION

All the specimens tested at 298 K failed in a ductile manner, as shown in the J-resistance curves and values given in Figure 1 for the toughness of the compact specimens. Similarly, the values of critical crack length shown in Figure 2 reflect this ductile behaviour; the value of 95 mm for the 30% cold worked and stress relieved specimen being in excellent agreement with that for specimens machined from pressure tube in the same metallurgical condition [22]. The shape of this latter curve appears linear over the range of heat treatments and corresponding values of CCL obtained. However, outside these ranges, the shape of the curve may alter, curving towards zero and perhaps becoming less steep as the toughness at 1.5 mm crack length exceeds 400 kN/m. For the present investigation, however, the linearity of this behaviour may prove useful from an engineering viewpoint.

Turning now to Figure 4, the relationship between toughness at 1.5 mm crack extension and the void diameter is also linear over the range investigated.

Thus, by plotting the void diameter against the CCL, a very useful engineering relationship may result, as shown in Figure 7. This is the ability to predict the critical crack length of Zr-Nb pressure tubes evolves from a knowledge of the void diameter in the stable crack growth region of a small, 17 mm compact test specimen.

The crack initiation toughness against stretch zone width relationship shown in Figure 3 has somewhat less appeal than does Figure 4 and Figure 7, simply because the predictive capability in the engineering sense from such a relationship may be considered to be limited. The designer may well be more interested in knowing how much crack extension can be tolerated in the CCL sense, rather than knowing the blunting capabilities of sharp cracks under tensile opening.

Much attention has been paid to the "void diameter" in the experimental approach. Examination of Figures 5 and 6 illustrates the need for both SEM and optical microscopy of the fracture surface in deciding which characteristic feature of the fracture surface and the microstructure gives rise to the void diameter which is appropriate for a given ductile fracture process. In Figure 5, the void size which is appropriate is that which corresponds to the find hydrides which act as void nuclei in this matrix.

In Figure 6, the appropriate void size is that which corresponds to regions of material which have been "sheared out" of the fracture surface as a consequence of easy separation along the massive hydride-matrix interfaces.

This concept of attributing ductile fracture to events involving a "major void diameter" was first proposed by Firrao [10] and the observations and measurements made have been in keeping with this concept for defining a microstructural feature which characterizes the ductile fracture mechanism of Zr-Nb subjected to various heat-treatments.

Clearly the magnitude of the "major void diameter" varies with microstructure. In Figure 5 the major void diameter is of the order of 12 microns, whereas in Figure 6, it is of the order of 36 microns. The smaller the value of "major void diameter", the greater the crack growth toughness.

CONCLUSIONS

Heat treatment significantly influences the fracture toughness of Zr-Nb.

For the conditions investigated, the toughness at 1.5 mm stable crack extension varied over the range 100 kN/m to 350 kN/m and resulted in tube critical crack lengths from 60 mm to 100 mm. Careful measurement of appropriate void diameters in these 17 mm compact specimens, which all failed by ductile fracture at 298 K, gave rise to a linear relationship between void diameter and critical crack length.

Thus, by determining microstructural features which characterize the mechanism of ductile fracture, a powerful design guide evolves which allows the prediction of the critical crack length for pressure tube to be determined from a knowledge of the void diameter in the stable crack growth region of small-scale specimens.

ACKNOWLEDGEMENTS

I am grateful to Mr. J. Watters, Mr. R. Bowden and Mrs. Ann Timmins for their contributions to the experimental work and to Dr. C. E. Ells for his comments on the manuscript. The specimens were tested at AECL, Chalk River.

REFERENCES

(1) A.S.T.M. STP 824, 1984.
(2) A.S.T.M. STP 754, 1982.
(3) A.S.T.M. STP 681, 1979.
(4) A.S.T.M. STP 633, 1977.
(5) A.S.T.M. STP 551, 1971.
(6) A.S.T.M. STP 939, 1987.
(7) Garrison, W. M., and Moody, N. R., Acta Metal., vol. 48, 1987, p. 1035.
(8) Thomson, A. W., Acta Metal., vol. 31, 1983, p. 1517.
(9) Knott, J. F., "Fundamentals of Fracture Mechanics" Butterworths, London, 1973.
(10) Firrao , D., et alia, ICF 7, Houston, Proceedings, 1989, p. 2483.
(11) A.S.T.M. Standard E813-81 "J_{1C} , A Measure of Fracture Toughness".
(12) Chow, C. K., and Simpson, L. A., A.S.T.M. STP 945, 1985, p. 419.
(13) Folias, E. S., Engineering Fracture Mechanics, vol. 2, 1970, p. 151.
(14) Kiefner, J. F., et alia, A.S.T.M. STP 536, 1973, p. 461.
(15) Simpson, L. A., A.E.C.L. Report AECL-6805, 1981.
(16) Northwood, D., and Lim, D., Canadian Metallurgical Quarterly, vol. 18, 1979, p. 441.

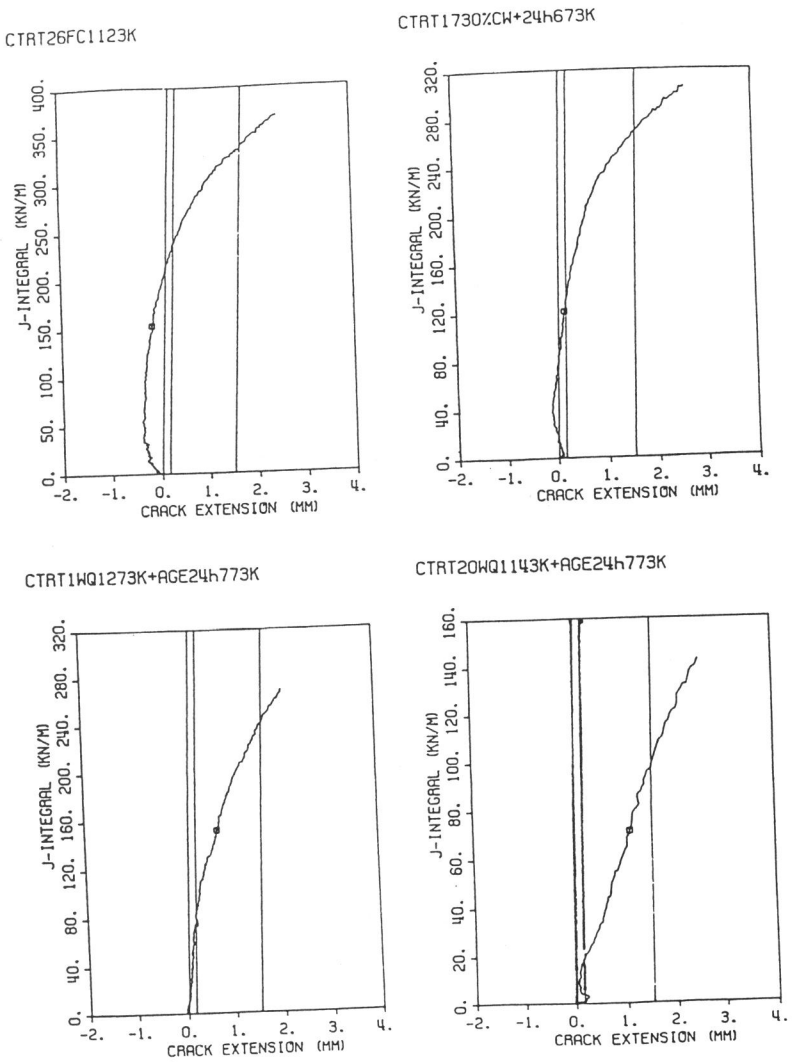

FIGURE 1: J-Resistance Curves for the four heat-treated conditions investigated.

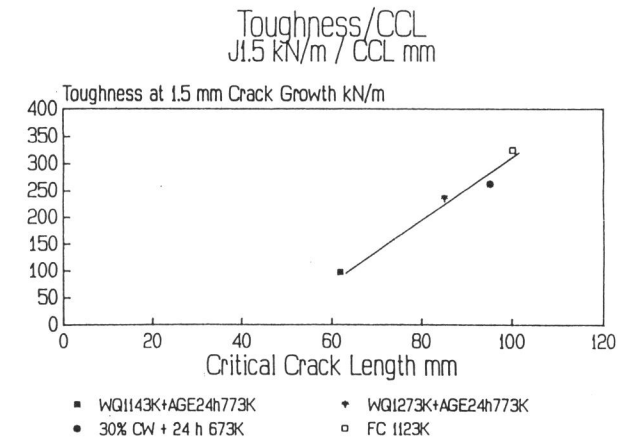

Zr-2.5 wt.% Nb Sheet Compacts

FIGURE 2: Effect of Toughness at 1.5 mm Stable Crack Growth on the Critical Crack Length of Pressure Tubes Heat-treated as shown

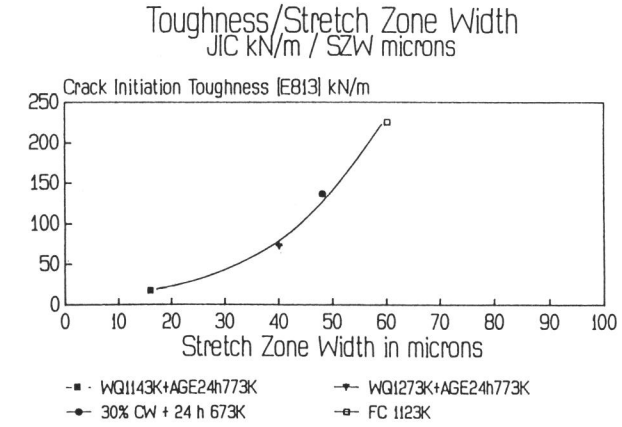

Zr-2.5 wt.% Nb Sheet Compacts
SZW measured at 60 degree tilt

FIGURE 3: Effect of J_{IC} on Stretch Zone Width for various Heat-treatments

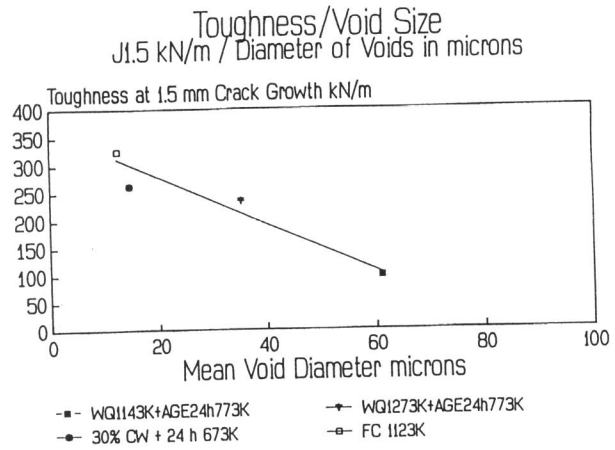

Zr-2.5 wt.% Nb Sheet Compacts

FIGURE 4: Effect of Toughness at 1.5 mm Stable Crack Growth on the Mean Void Diameter in the Stable Crack Growth region

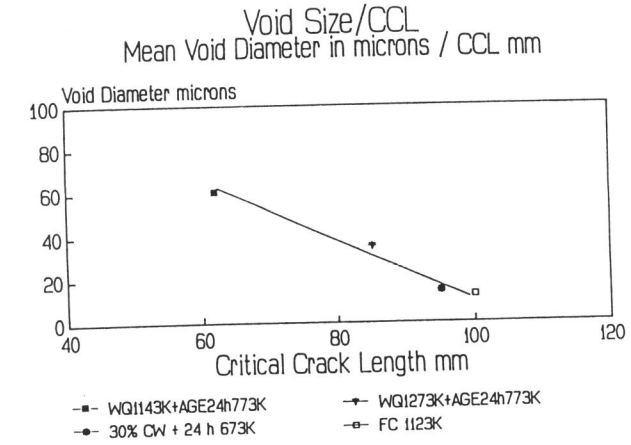

Zr-2.5 wt.% Nb Sheet Compacts

FIGURE 7: Effect of Mean Void Diameter on the Critical Crack Length of Heat-treated Pressure Tube

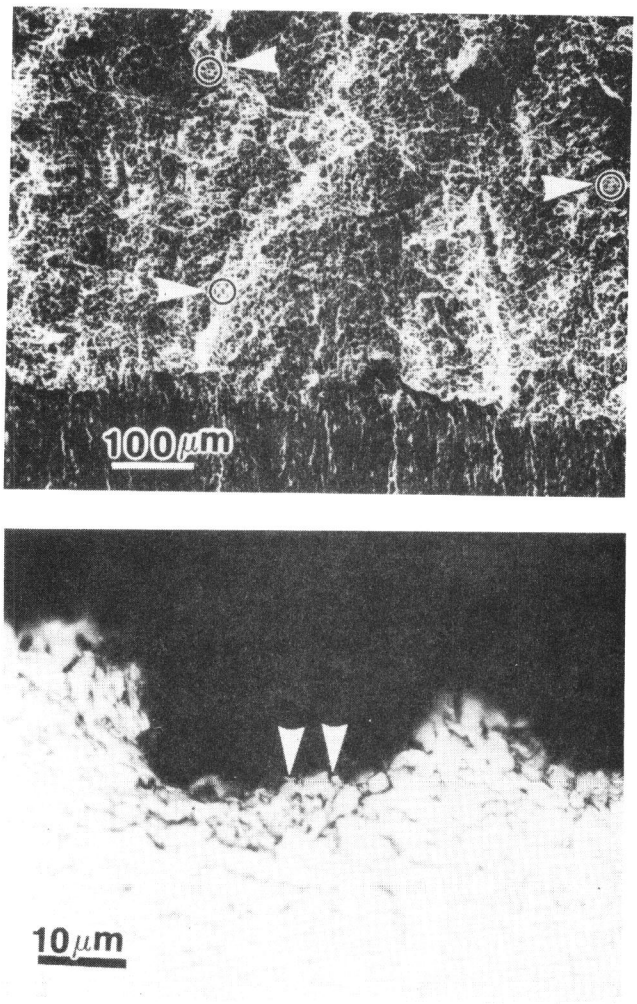

Figure 5: (a) Scanning electron micrograph showing ductile fracture. The arrowed circles enclose approximately 3 major voids to give a major void size of 12 microns.
(b) Optical micrograph of a section cut through the stable crack growth region with the arrows indicating intergranular hydrides as the dominant microstructural feature causing the major voids. The hydride filaments are about 12 microns in length.

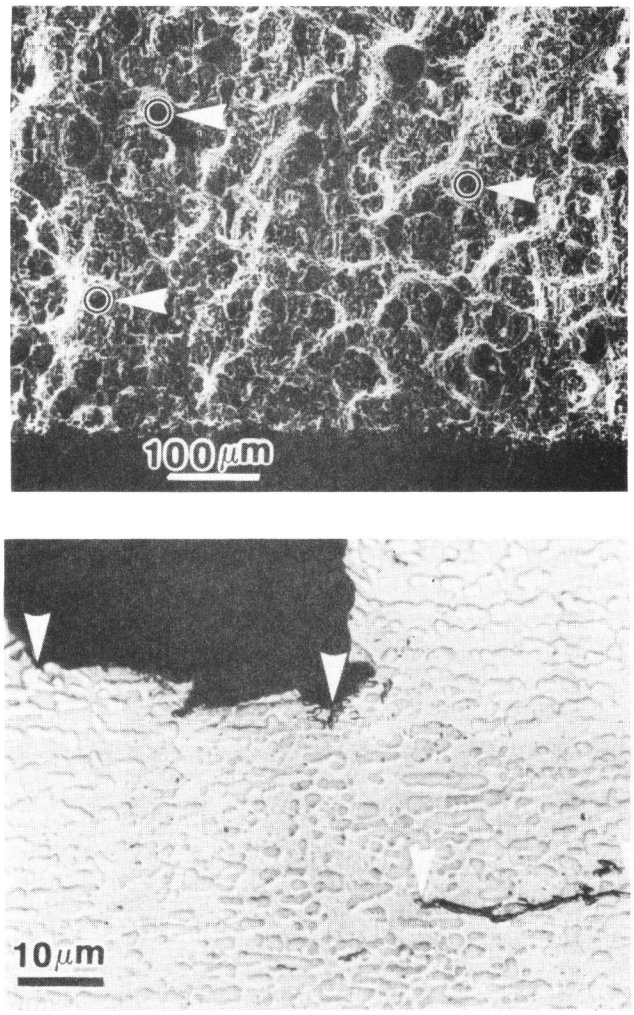

Figure 6: (a) Scanning electron micrograph showing ductile fracture. The arrowed circles are of the same diameter as the major voids of approximately 36 microns. (b) Optical micrograph of a section cut through the stable crack growth region with the arrows showing massive hydrides and a sheared out hydride interface indicating massive hydrides as the dominant microstructural feature causing the major voids. The hydride filaments are about 36-40 microns in length.